1

Crystal Structures

Our general objective in this book is to understand the macroscopic properties of solids on a microscopic level. In view of the many particles in solids, coming up with any microscopic description appears to be a daunting task. It is clearly impossible to solve the equations of motion (classical or quantum-mechanical) of the particles. Fortunately, it turns out that solids are often crystalline, with the atoms arranged on a regular lattice, and this symmetry permits us to solve microscopic models despite the vast number of particles involved. In a way, this situation is similar to atomic physics where the key to a quantum-mechanical description is the spherical symmetry of the atom. We will often imagine a macroscopic solid as one **single crystal**, a perfect lattice of atoms without any defects whatsoever. While it may seem that such perfect crystals are not particularly relevant for real materials, this is in fact not the case. Many solids are actually composed of small crystalline grains. Such solids are called **polycrystalline**, in contrast to a macroscopic single crystal, but the number of atoms within a perfect crystalline environment in them is still very large compared to the number of atoms on the **grain boundary**. For instance, for a grain size on the order of 1000^3 atomic distances, only about 0.1% of all atoms are at the grain boundaries.

There are, however, also solids that are not crystalline. These are called **amorphous**. The amorphous state is characterized by the absence of any long-range order. There may exist, however, a degree of short-range order between the atoms.

This chapter is divided into three parts. In the first part, we define some basic mathematical concepts needed to describe crystals. We keep things simple and mostly use two-dimensional examples to illustrate the ideas. In the second part, we discuss common crystal structures. For the moment, we will not ask *why* the atoms bind together in the way they do – this topic will be discussed in Chapter 2. Finally, we delve into a more detailed discussion of X-ray diffraction, the experimental technique that can be used to determine the microscopic structure of crystals. X-ray diffraction is used not only in solid state physics but also for a wide range of problems in nanotechnology and structural biology.

Solid State Physics: An Introduction, Third Edition. Philip Hofmann.

1.1 General Description of Crystal Structures

Our description of crystals starts with the mathematical definition of the **lattice**. A lattice is a set of regularly spaced points with positions defined as multiples of generating vectors. In two dimensions, a lattice can be defined as all the points that can be reached by the vectors $\mathbf{R}$, created from two non-collinear vectors $\mathbf{a_1}$ and $\mathbf{a_2}$ as

$$\mathbf{R} = m\mathbf{a_1} + n\mathbf{a_2}, \tag{1.1}$$

where n and m are integers. In three dimensions, the corresponding definition is

$$\mathbf{R} = m\mathbf{a_1} + n\mathbf{a_2} + o\mathbf{a_3}. \tag{1.2}$$

Such a lattice of points is also called a **Bravais lattice**. The number of possible Bravais lattices with different symmetries is limited to 5 in two dimensions and to 14 in three dimensions. An example of a two-dimensional Bravais lattice is given in Figure 1.1. The lengths of the vectors $\mathbf{a_1}$ and $\mathbf{a_2}$ are often called the **lattice constants**.

Having defined the Bravais lattice, we move on to the definition of the **primitive unit cell**. By this we denote any volume of space that, when translated through all the vectors of the Bravais lattice, will fill space without overlap and without leaving any voids. The primitive unit cell of a lattice contains only one lattice point. It is also possible to define **nonprimitive unit cells** containing several lattice points. These fill space without leaving voids when translated through a subset of the Bravais lattice vectors. Possible choices of a unit cell for a two-dimensional rectangular Bravais lattice are illustrated in Figure 1.2. It is evident from the figure that a nonprimitive unit cell has to be translated by a multiple of one (or two) lattice vectors to fill space without voids and overlap. A special choice of the primitive unit cell is the **Wigner–Seitz cell**, which is also shown in Figure 1.2. It is the region of space that is closer to one given lattice point than to any other.

The last definition we need in order to describe an actual crystal is that of a **basis**. The basis describes the items we "put" on the lattice points, that is, the building blocks for the real crystal. The basis can consist of one or several atoms, or even of complex molecules as in the case of protein crystals. Different cases are illustrated in Figure 1.3.

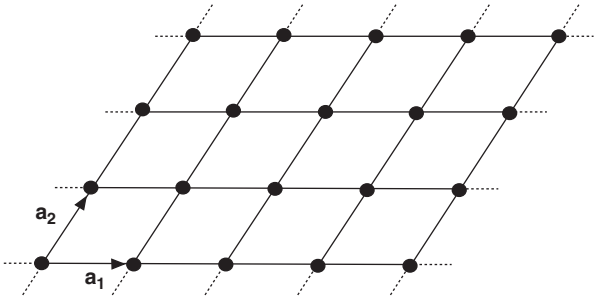

Figure 1.1 A two-dimensional Bravais lattice.

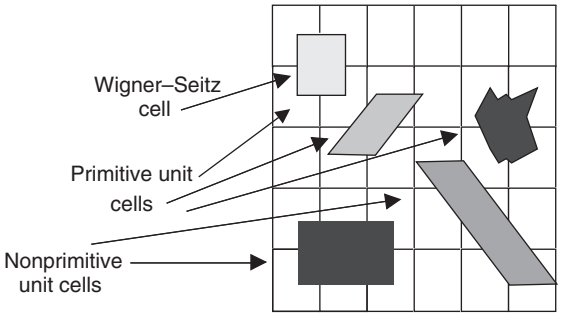

Figure 1.2 Illustration of (primitive and nonprimitive) unit cells and of the Wigner–Seitz cell for a rectangular two-dimensional lattice.

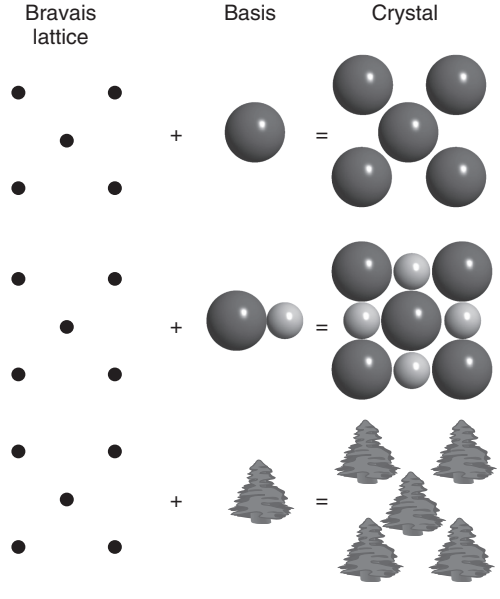

Figure 1.3 A two-dimensional Bravais lattice with different choices for the basis.

Finally, we add a remark about symmetry. So far, we discussed only **translational symmetry**. However, a real crystal may also exhibit **point symmetry**. Compare the structures in the middle and the bottom of Figure 1.3. The former structure possesses a number of symmetry elements that are missing in the latter – for example, mirror lines, a rotational axis, and inversion symmetry. The knowledge of such symmetries can be very useful for the description of crystal properties.

1.2 Some Important Crystal Structures

After this rather formal treatment, we look at a number of common crystal structures for different types of solids, such as metals, ionic solids, or covalently bonded solids. In Chapter 2, we will take a closer look at the details of the bonding in these types of solids.

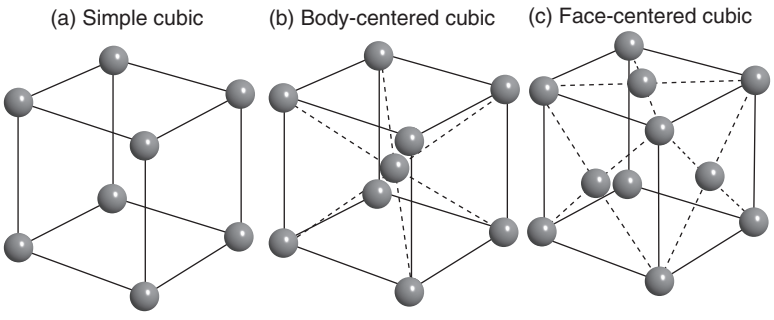

Figure 1.4 (a) Simple cubic structure; (b) body-centered cubic structure; and (c) face-centered cubic structure. Note that the spheres are depicted much smaller than in the situation of most dense packing and not all of the spheres on the faces of the cube are shown in (c).

1.2.1 Cubic Structures

We begin with one of the simplest crystal structures possible, the **simple cubic structure** shown in Figure 1.4a. This structure is not very common among elemental solids, but it is an important starting point for understanding many other structures. Only one chemical element (polonium) is found to crystallize in the simple cubic structure. The structure is unfavorable because of its openness – there are many voids, if we think of the atoms as solid spheres in contact with each other. In metals, which are the most common elemental solids, directional bonding is not important, and a close packing of the atoms is usually favored. We will learn more about this in the next chapter. For covalent solids, on the other hand, directional bonding *is* important, but six bonds extending from the same atom in an octahedral configuration is highly uncommon in elemental solids.

The packing density of the cubic structure is improved in the **body-centered cubic** (bcc) and **face-centered cubic** (fcc) structures that are also depicted in Figure 1.4. In fact, the fcc structure has the highest possible packing density for identical spheres, as we shall see later. These two structures are very common – 17 elements crystallize in the bcc structure and 24 elements in the fcc structure. Note that the simple cubic structure ist the only one for which the cube is identical with the Bravais lattice. While the cube is also a unit cell for the bcc and fcc lattices, ist it not the primitive unit cell in these cases. Still, both structures are Bravais lattices with a basis containing one atom, but the vectors spanning these Bravais lattices are not the edges of the cube.

Cubic structures with a more complex basis than a single atom are also important. Figure 1.5 shows the structures of the ionic crystals CsCl and NaCl, which are both cubic with a basis containing two atoms. For CsCl, the structure can be thought of as two simple cubic structures stacked into each other. For NaCl, it consists of two fcc lattices stacked into each other. Which structure is preferred for such ionic crystals depends on the relative size of the positive and negative ions.

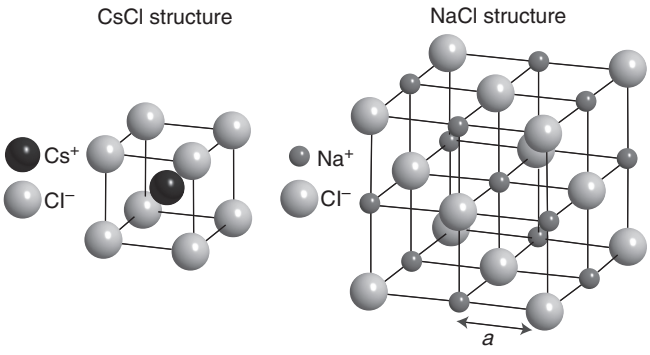

Figure 1.5 Structures of CsCl and NaCl. The spheres are depicted much smaller than in the situation of dense packing, but the relative size of the different ions in each structure is correct.

1.2.2 Close-Packed Structures

Many metals prefer structural arrangements where the atoms are packed as closely as possible. In two dimensions, the closest possible packing of atoms (i.e. spheres) is the hexagonal structure shown on the left-hand side of Figure 1.6. To build a three-dimensional close-packed structure, one adds a second layer as in the middle of Figure 1.6. Now there are two possibilities, however, for adding a third layer. We can either put the atoms in the "holes" just on top of the first-layer atoms, or we can put them into the other type of "holes." The result are two different crystal structures. The first has an ABABAB… layer stacking sequence, the second an ABCABCABC… layer stacking sequence. Both have exactly the same packing density with the spheres filling about 74% of the total volume. The former structure is called the **hexagonal close-packed structure** (hcp), and the latter turns out to be the fcc structure we already know. An alternative sketch of the hcp structure is shown in Figure 1.16b. The fcc and hcp structures are very common in elemental metals, 36 chemical elements crystallizing in hcp and 24 in fcc lattices. These structures also maximize the number of nearest neighbors for a given atom, the so-called **coordination number**. For both the fcc and the hcp lattices, the coordination number is 12.

Figure 1.6 Close packing of spheres leading to the hcp and fcc structures.

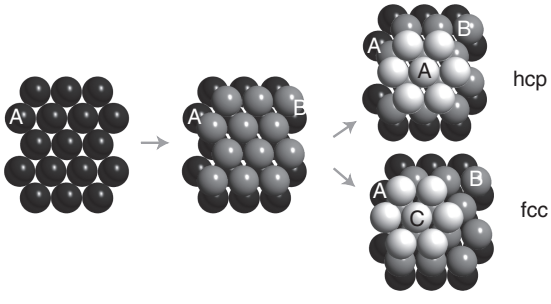

It is as yet an unresolved question why not all metals crystallize in the fcc or hcp structures, if coordination is indeed so important. Whereas a prediction of the actual structure for a given element is not possible on the basis of simple arguments, we can identify some factors that play a role. For example, structures that are not optimally packed, such as the bcc structure, have a lower coordination number, but they bring the second-nearest neighbors much closer to a given atom than in the close-packed structures. Another important consideration is that the bonding situation is often not quite so simple, particularly in **transition metals**. In these, bonding is not only achieved through the delocalized s and p valence electrons as in **simple metals**, but also by the more localized d electrons. Bonding through the latter results in a much more directional character so that not only the close packing of the atoms is important.

The structures of many ionic solids can also be viewed as "close-packed" in some sense. One can derive these structures by treating the ions as hard spheres that have to be packed as closely to each other as possible.

1.2.3 Structures of Covalently Bonded Solids

In covalent structures, the valence electrons of the atoms are not completely delocalized but shared between neighboring atoms, and bond lengths and directions are far more important than the packing density. Prominent examples are graphene, graphite, and diamond as displayed in Figure 1.7. Graphene is a single sheet of carbon atoms in a honeycomb lattice structure. It is a truly two-dimensional solid with a number of remarkable properties – so remarkable, in fact, that their discovery has lead to the 2010 Nobel prize in physics being awarded to A. Geim and K. Novoselov. The carbon atoms in graphene are connected through a network of sp^2 hybrid bonds enclosing angles of 120°. The parent material of graphene is graphite, which consists of a stack of graphene sheets that are weakly bonded to each other. In fact, graphene can be isolated from graphite by peeling off flakes with a piece of scotch tape. In diamond, the carbon atoms form sp^3-type bonds and each atom has four nearest neighbors in a tetrahedral configuration. Interestingly, the diamond structure can also be described as an fcc Bravais lattice with a basis of two atoms.

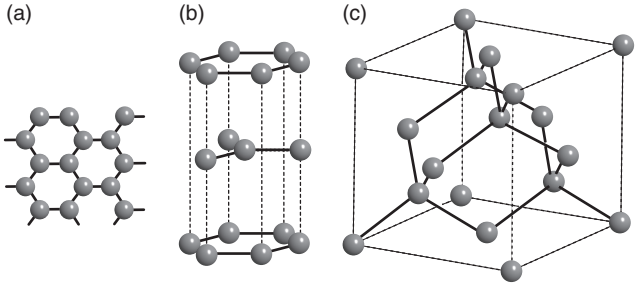

Figure 1.7 Structures for (a) graphene, (b) graphite, and (c) diamond. Bonds from sp^2 and sp^3 orbitals are displayed as solid lines.

The diamond structure is also found for Si and Ge. Many other isoelectronic materials (i.e. materials with the same total number of valence electrons), such as SiC, GaAs, or InP, also crystallize in a diamond-like structure but with each element on a different fcc sublattice.

1.3 Crystal Structure Determination

After having described different crystal structures, the question is of course how to determine these structures in the first place. By far the most important technique for this is X-ray diffraction. In fact, the importance of this technique extends far beyond solid state physics, as it has become an essential tool for fields such as structural biology as well. In biology, the idea is that you can derive the structure of a given protein by trying to crystallize it and then use the powerful methodology of X-ray diffraction to determine its structure. In addition, we will also use X-ray diffraction as a motivation to extend our formal description of structures.

1.3.1 X-Ray Diffraction

X-rays interact rather weakly with matter. A description of X-ray diffraction can therefore be restricted to single scattering, meaning that we limit our analysis to the case that X-rays incident upon a crystal sample get scattered not more than once (most are not scattered at all). This is called the **kinematic approximation;** it greatly simplifies matters and is used throughout the treatment in this book. Furthermore, we will assume that the X-ray source and detector are placed very far away from the sample so that the incoming and outgoing waves can be treated as plane waves. X-ray diffraction of crystals was discovered and described by M. von Laue in 1912. Also in 1912, W. L. Bragg came up with an alternative description that is considerably simpler and will serve as a starting point for our analysis.

1.3.1.1 Bragg Theory

Bragg treated the problem as the reflection of the incident X-rays at flat crystal planes. These planes could, for example, be the close-packed planes making up fcc and hcp crystals, or they could be alternating Cs and Cl planes making up the CsCl structure. At first glance, the physical justification for this picture seems somewhat dubious, because the crystal planes appear certainly not "flat" for X-rays with wavelengths on the order of atomic spacing. Nevertheless, the description proved highly successful, and we shall later see that it is actually a special case of the more complex Laue description of X-ray diffraction.

Figure 1.8 shows the geometrical considerations behind the Bragg description. A collimated beam of monochromatic X-rays hits the crystal. The intensity of diffracted X-rays is measured *in the specular direction*. The angles of incidence and emission are $90^\circ - \Theta$. The condition for constructive interference is that the path length difference between the X-rays reflected from one layer and the next layer is

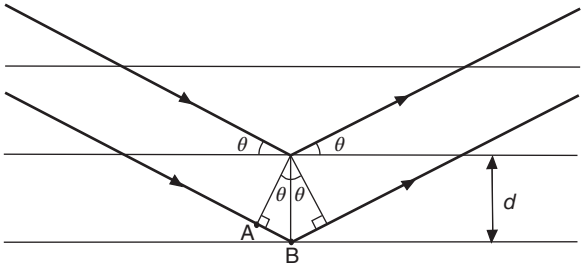

Figure 1.8 Construction for the derivation of the Bragg condition. The horizontal lines represent the crystal lattice planes that are separated by a distance d. The heavy lines represent the X-rays.

an integer multiple of the wavelength λ. In the figure, this means that $2AB = n\lambda$, where AB is the distance between points A and B and n is a natural number. On the other hand, we have $\sin\theta = AB/d$, which leads us to the **Bragg condition**

$$n\lambda = 2d\sin\theta. \tag{1.3}$$

It is obvious that if this condition is fulfilled for one specific layer and the layer below it, then it will also be fulfilled for any number of layers with identical spacing. In fact, the X-rays penetrate very deeply into the crystal so that thousands of layers contribute to the reflection. This results in very sharp maxima in the diffracted intensity, similar to the situation for an optical grating with many lines. The Bragg condition can obviously only be fulfilled for $\lambda < 2d$, putting an upper limit on the wavelength of the X-rays that can be used for crystal structure determination.

1.3.1.2 Lattice Planes and Miller Indices

Obviously, the Bragg condition will be satisfied not only for a special kind of lattice plane in a crystal, such as the hexagonal planes in an hcp crystal, but for all possible parallel planes in a structure. Thus, we need a more precise definition of the term **lattice plane**. It proves useful to define a lattice plane as a plane containing at least three non-collinear lattice points of a given Bravais lattice. If it contains three points, it will actually contain infinitely many because of the translational symmetry of the lattice. Examples for lattice planes in a simple cubic structure are shown in Figure 1.9.

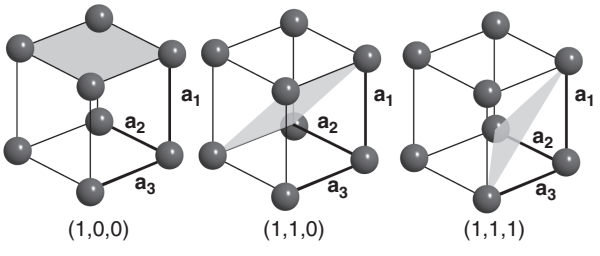

Figure 1.9 Three different lattice planes in the simple cubic structure characterized by their Miller indices.

Following this definition, all lattice planes can be characterized by a set of three integers, the so-called **Miller indices**. We derive them in three steps:

1) We find the intercepts of the specific plane at hand with the crystallographic axes in units of the lattice vectors, for example, $(1, \infty, \infty)$ for the leftmost plane in Figure 1.9.
2) We take the "reciprocal value" of these three numbers. For our example, this gives $(1,0,0)$.
3) We multiply the numbers obtained in this manner with some factor so that we arrive at the smallest set of integers having the same ratio. In the example given, this is not necessary as all number are already integers.

Such a set of three integers can then be used to denote any given lattice plane. Later, we will encounter a different and more elegant definition of the Miller indices.

In practice, the X-ray diffraction peaks are so sharp that it is difficult to align and move the sample so that the incoming and reflected X-rays lie in a plane normal to a certain crystal plane. An elegant way to circumvent this problem is to use a powder consisting of very small crystals instead of a large single crystal. This will not only ensure that some of the many crystals are oriented correctly to get constructive interference from a certain set of crystal planes, it will also automatically yield the interference pattern for all possible crystal planes.

1.3.1.3 General Diffraction Theory

The Bragg theory for X-ray diffraction is useful for extracting the distances between lattice planes in a crystal, but it has its limitations. Most importantly, it does not provide any information on what the lattice actually consists of, that is, the basis. Also, the fact that the X-rays are described as being reflected by planes is physically somewhat obscure. In the following, we will therefore discuss a more general description of X-ray diffraction that goes back to M. von Laue.

The physical process leading to X-ray scattering is that the electromagnetic field of the X-rays forces the electrons in the material to oscillate with the same frequency as that of the field. The oscillating electrons then emit new X-rays that give rise to an interference pattern. For the following discussion, however, it is merely important that something scatters the X-rays, not what it is.

It is highly beneficial to use the complex notation for describing the electromagnetic X-ray waves. For the electric field, a general plane wave can be written as

$$\boldsymbol{\mathcal{E}}(\mathbf{r}, t) = \boldsymbol{\mathcal{E}}_0 \, \mathrm{e}^{\mathrm{i}\mathbf{k}\cdot\mathbf{r} - \mathrm{i}\omega t}. \tag{1.4}$$

The wave vector $\mathbf{k}$ points in the direction of the wave propagation with a length of $2\pi/\lambda$, where λ is the wavelength. The convention is that the physical electric field

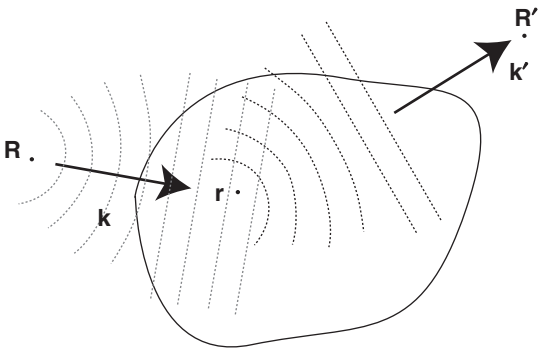

Figure 1.10 Illustration of X-ray scattering from a sample. The source and detector for the X-rays are placed at **R** and **R′**, respectively. Both are very far away from the sample.

is obtained as the real part of the complex field and the intensity of the wave is obtained as

$$I(\mathbf{r}) = \left|\mathcal{E}_0\, \mathrm{e}^{\mathrm{i}\mathbf{k}\cdot\mathbf{r}-\mathrm{i}\omega t}\right|^2 = \left|\mathcal{E}_0\right|^2. \tag{1.5}$$

Consider now the situation depicted in Figure 1.10. The source of the X-rays is far away from the sample at the position **R** so that the X-ray wave at the sample can be described as a plane wave. The electric field at a point **r** in the crystal at time t can be written as

$$\mathcal{E}(\mathbf{r}, t) = \mathcal{E}_0\, \mathrm{e}^{\mathrm{i}\mathbf{k}\cdot(\mathbf{r}-\mathbf{R})-\mathrm{i}\omega t}. \tag{1.6}$$

Before we proceed, we can drop the absolute amplitude $\mathcal{E}_0$ from this expression because we are only interested in relative phase changes. The field at point **r** is then

$$\mathcal{E}(\mathbf{r}, t) \propto \mathrm{e}^{\mathrm{i}\mathbf{k}\cdot(\mathbf{r}-\mathbf{R})}\, \mathrm{e}^{-\mathrm{i}\omega t}. \tag{1.7}$$

A small volume element $\mathrm{d}V$ located at **r** will give rise to scattered waves in all directions. The direction we are interested in is that towards the detector, which we assume to be placed at position $\mathbf{R}'$, in the direction of a second wave vector $\mathbf{k}'$. We assume that the amplitude of the wave scattered in this direction will be proportional to the incoming field from Eq. (1.7) and to a factor $\rho(\mathbf{r})$ describing the scattering probability and scattering phase. We already know that the scattering of X-rays proceeds via the electrons in the material, and for our purpose, we can view $\rho(\mathbf{r})$ as the electron concentration in the solid. For the field at the detector, we obtain

$$\mathcal{E}(\mathbf{R}', t) \propto \mathcal{E}(\mathbf{r}, t)\rho(\mathbf{r})\, \mathrm{e}^{\mathrm{i}\mathbf{k}'\cdot(\mathbf{R}'-\mathbf{r})}. \tag{1.8}$$

Again, we have assumed that the detector is very far away from the sample so that the scattered wave at the detector can be written as a plane wave. Inserting Eq. (1.7) gives the field at the detector as

$$\mathcal{E}(\mathbf{R}', t) \propto \mathrm{e}^{\mathrm{i}\mathbf{k}\cdot(\mathbf{r}-\mathbf{R})}\rho(\mathbf{r})\, \mathrm{e}^{\mathrm{i}\mathbf{k}'\cdot(\mathbf{R}'-\mathbf{r})}\, \mathrm{e}^{-\mathrm{i}\omega t} = \mathrm{e}^{\mathrm{i}(\mathbf{k}'\cdot\mathbf{R}'-\mathbf{k}\cdot\mathbf{R})}\rho(\mathbf{r})\, \mathrm{e}^{\mathrm{i}(\mathbf{k}-\mathbf{k}')\cdot\mathbf{r}}\, \mathrm{e}^{-\mathrm{i}\omega t}. \tag{1.9}$$

We drop the first factor that does not contain **r** and will thus not play a role for the interference of X-rays emitted from different positions in the sample. The total wave field at the detector can finally be calculated by integrating over the entire volume

V of the crystal. As the detector is far away from the sample, the wave vector $\mathbf{k}'$ is essentially the same for all points in the sample. The result is therefore

$$\mathcal{E}(\mathbf{R}', t) \propto \mathrm{e}^{-\mathrm{i}\omega t} \int_V \rho(\mathbf{r})\, \mathrm{e}^{\mathrm{i}(\mathbf{k}-\mathbf{k}')\cdot\mathbf{r}}\, \mathrm{d}V. \tag{1.10}$$

In most cases, it will only be possible to measure the intensity of the X-rays and not the field amplitude. This intensity is given by

$$I(\mathbf{K}) \propto \left| \mathrm{e}^{-\mathrm{i}\omega t} \int_V \rho(\mathbf{r})\, \mathrm{e}^{\mathrm{i}(\mathbf{k}-\mathbf{k}')\cdot\mathbf{r}}\, \mathrm{d}V \right|^2 = \left| \int_V \rho(\mathbf{r})\, \mathrm{e}^{-\mathrm{i}\mathbf{K}\cdot\mathbf{r}}\, \mathrm{d}V \right|^2, \tag{1.11}$$

where we have introduced the so-called scattering vector $\mathbf{K} = \mathbf{k}' - \mathbf{k}$, which is just the difference of the outgoing and incoming wave vectors. Note that although the direction of the wave vector $\mathbf{k}'$ for the scattered waves is different from that of the incoming wave $\mathbf{k}$, their lengths are the same because we consider elastic scattering only.

Equation (1.11) is our final result. It relates the measured intensity to the electron concentration in the sample. Except for very light elements, most of the electrons are located close to the ion cores and the electron concentration that scatters the X-rays is essentially identical to the geometrical arrangement of the atomic cores. Hence, Eq. (1.11) can be used for the desired structure determination. To this end, one could try to measure the intensity as a function of scattering vector $\mathbf{K}$ and to infer the structure from the result. This is a formidable task, however. It is greatly simplified by the fact that the specimen under investigation is a crystal with a periodic lattice. In the following, we introduce the mathematical tools and concepts that are needed to exploit the crystalline structure in the analysis. The most important of these is the so-called reciprocal lattice.

1.3.1.4 The Reciprocal Lattice

The concept of the reciprocal lattice is fundamental to solid state physics because it permits us to exploit crystal symmetry in the analysis of many problems. Here, we will use it to describe X-ray diffraction from periodic structures and we will continue to meet it again in the following chapters. Unfortunately, the meaning of the reciprocal lattice turns out to be difficult to grasp. We will start out with a formal definition and provide some of its mathematical properties. We then go on to discuss the meaning of the reciprocal lattice before we come back to X-ray diffraction. The full importance of the concept will become apparent in the course of this book.

For a given Bravais lattice

$$\mathbf{R} = m\mathbf{a_1} + n\mathbf{a_2} + o\mathbf{a_3}, \tag{1.12}$$

we define the reciprocal lattice as the set of vectors $\mathbf{G}$ for which

$$\mathbf{R} \cdot \mathbf{G} = 2\pi\, l, \tag{1.13}$$

where l is an integer. Equivalently, we could require that

$$\mathrm{e}^{\mathrm{i}\mathbf{G}\cdot\mathbf{R}} = 1. \tag{1.14}$$

Note that this equation must hold for *any* choice of the lattice vector **R** and reciprocal lattice vector **G**. We can write any **G** as the linear combination of three vectors

$$\mathbf{G} = m'\,\mathbf{b_1} + n'\,\mathbf{b_2} + o'\,\mathbf{b_3}, \tag{1.15}$$

where m', n' and o' are integers. The reciprocal lattice is also a Bravais lattice. The vectors $\mathbf{b_1}$, $\mathbf{b_2}$, and $\mathbf{b_3}$ spanning the reciprocal lattice can be constructed explicitly from the lattice vectors [1]

$$\mathbf{b}_1 = 2\pi\frac{\mathbf{a}_2 \times \mathbf{a}_3}{\mathbf{a}_1 \cdot (\mathbf{a}_2 \times \mathbf{a}_3)}, \quad \mathbf{b}_2 = 2\pi\frac{\mathbf{a}_3 \times \mathbf{a}_1}{\mathbf{a}_1 \cdot (\mathbf{a}_2 \times \mathbf{a}_3)}, \quad \mathbf{b}_3 = 2\pi\frac{\mathbf{a}_1 \times \mathbf{a}_2}{\mathbf{a}_1 \cdot (\mathbf{a}_2 \times \mathbf{a}_3)}. \tag{1.16}$$

From this, one can derive the simple but useful property[2]

$$\mathbf{a}_i \cdot \mathbf{b}_j = 2\pi\,\delta_{ij}, \tag{1.17}$$

which can easily be verified. Equation (1.17) can then be used to verify that the reciprocal lattice vectors defined by Eqs. (1.15) and (1.16) do indeed fulfill the fundamental property of Eq. (1.13) defining the reciprocal lattice (see also Problem 1.6).

Another way to view the vectors of the reciprocal lattice is as wave vectors that yield plane waves with the periodicity of the Bravais lattice, because

$$\mathrm{e}^{\mathrm{i}\mathbf{G}\cdot\mathbf{r}} = \mathrm{e}^{\mathrm{i}\mathbf{G}\cdot\mathbf{r}}\,\mathrm{e}^{\mathrm{i}\mathbf{G}\cdot\mathbf{R}} = \mathrm{e}^{\mathrm{i}\mathbf{G}\cdot(\mathbf{r}+\mathbf{R})}. \tag{1.18}$$

Using the reciprocal lattice, we can finally define the **Miller indices** in a much simpler way: The Miller indices (i, j, k) define a plane that is perpendicular to the reciprocal lattice vector $i\mathbf{b_1} + j\mathbf{b_2} + k\mathbf{b_3}$ (see Problem 1.9).

1.3.1.5 The Meaning of the Reciprocal Lattice

We have now defined the reciprocal lattice in a proper way, and we will give some simple examples of its usefulness. The most important feature of the reciprocal lattice is that it facilitates the description of functions with the same periodicity as that of the lattice. To see this, consider a one-dimensional lattice, a chain of points with a lattice constant a (Fig. 1.11). We are interested in a function with the periodicity of the lattice, such as the electron concentration $\rho(x)$ along the chain, $\rho(x) = \rho(x + a)$. We can write this as a Fourier series of the form

$$\rho(x) = C + \sum_{n=1}^{\infty} \left\{ C_n \cos(x\ 2\pi\ n/a) + S_n \sin(x\ 2\pi\ n/a) \right\} \tag{1.19}$$

with real coefficients C_n and S_n. The sum starts at $n = 1$, the constant C is therefore outside the summation. Using complex coefficients ρ_n, we can also write this in the more compact form

$$\rho(x) = \sum_{n=-\infty}^{\infty} \rho_n\,\mathrm{e}^{\mathrm{i}xn\,2\pi/a}. \tag{1.20}$$

---

1 The denominator is chosen to be the same for all three reciprocal lattice vectors, but note that the combination of dot product and cross product is "circular" such that $\mathbf{a}_1 \cdot (\mathbf{a}_2 \times \mathbf{a}_3) = \mathbf{a}_2 \cdot (\mathbf{a}_3 \times \mathbf{a}_1) = \mathbf{a}_3 \cdot (\mathbf{a}_1 \times \mathbf{a}_2)$.

2 δ_{ij} denotes Kronecker's delta, which is 1 for $i = j$ and zero otherwise.

To ensure that $\rho(x)$ is still a real function, we require that

$$\rho^*_{-n} = \rho_n, \tag{1.21}$$

that is, that the coefficient ρ_{-n} must be the complex conjugate of the coefficient ρ_n. This description is more elegant than the one with the sine and cosine functions. How is it related to the reciprocal lattice? In one dimension, the reciprocal lattice of a chain of points with lattice constant a is also a chain of points, now with spacing $2\pi/a$ [see Eq. (1.17)]. This means that we can write a general reciprocal lattice "vector" as

$$g = n\frac{2\pi}{a}, \tag{1.22}$$

where n is an integer. Exactly these reciprocal lattice "vectors" appear in Eq. (1.20). In fact, Eq. (1.20) is a sum of functions with a periodicity corresponding to the lattice vector, weighted by the coefficients ρ_n. Figure 1.11 illustrates these ideas by showing the lattice and reciprocal lattice for such a chain as well as two lattice-periodic functions, both in real space and as Fourier coefficients on the reciprocal lattice points. The advantage of describing these functions by the coefficients ρ_n is immediately obvious: Instead of giving $\rho(x)$ for *every* point in a range of $0 \leqslant x < a$, the Fourier description consists of just three numbers for the upper function and five numbers for the lower function. Actually, these even reduce to two and three numbers, respectively, because of Eq. (1.21).

The same ideas also work in three dimensions. In fact, one can use a Fourier sum for lattice-periodic properties that corresponds to Eq. (1.20). For the lattice-periodic electron concentration $\rho(\mathbf{r}) = \rho(\mathbf{r} + \mathbf{R})$, we get

$$\rho(\mathbf{r}) = \sum_{\mathbf{G}} \rho_{\mathbf{G}}\, \mathrm{e}^{\mathrm{i}\mathbf{G}\cdot\mathbf{r}}, \tag{1.23}$$

where $\mathbf{G}$ are the reciprocal lattice vectors.

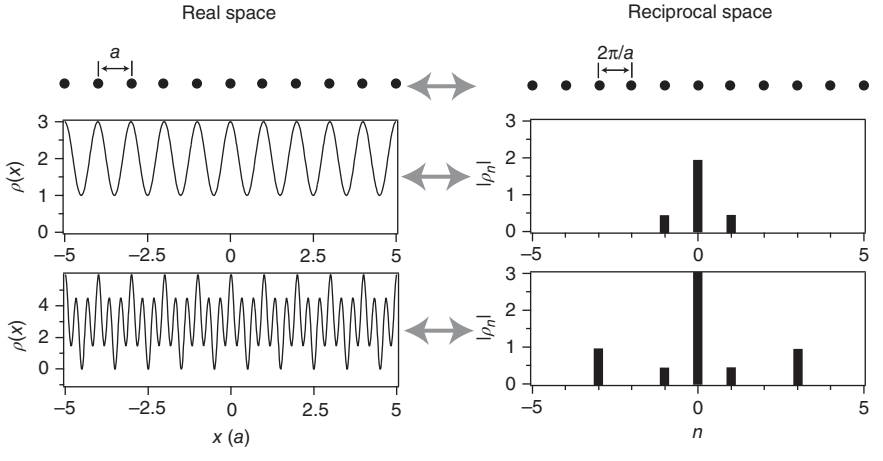

Figure 1.11 Top: A chain with a lattice constant a as well as its reciprocal lattice, a chain with a spacing of $2\pi/a$. Middle and bottom: Two lattice-periodic functions $\rho(x)$ in real space as well as their Fourier coefficients. The magnitude of the Fourier coefficients $|\rho_n|$ is plotted on the reciprocal lattice vectors they belong to.

Thus we have seen that the reciprocal lattice is very useful for describing lattice-periodic functions. But this is not the whole story: The reciprocal lattice can also simplify the treatment of waves in crystals in a very general sense. Such waves can be X-rays, elastic lattice distortions, or even electronic wave functions. We will come back to this point at a later stage.

1.3.1.6 X-Ray Diffraction from Periodic Structures

Turning back to the specific problem of X-ray diffraction, we can now exploit the fact that the electron concentration is lattice-periodic by inserting Eq. (1.23) in our expression from Eq. (1.11) for the diffracted intensity. This yields

$$I(\mathbf{K}) \propto \left| \sum_{\mathbf{G}} \rho_{\mathbf{G}} \int_V \mathrm{e}^{\mathrm{i}(\mathbf{G}-\mathbf{K})\cdot\mathbf{r}} \, \mathrm{d}V \right|^2 . \tag{1.24}$$

Let us inspect the integrand. The exponential represents a plane wave with a wave vector $\mathbf{G} - \mathbf{K}$. If the crystal is very big, the integration will average over the crests and troughs of this wave and the result of the integration will be very small (or zero for an infinitely large crystal). The only exception to this is the case where

$$\mathbf{K} = \mathbf{k}' - \mathbf{k} = \mathbf{G}, \tag{1.25}$$

that is, when the difference between incoming and scattered wave vector equals a reciprocal lattice vector. In this case, the exponential in the integral is 1, and the value of the integral is equal to the volume of the crystal. Equation (1.25) is often called the **Laue condition**. It is central to the description of X-ray diffraction from crystals in that it describes the condition for the observation of constructive interference.

Looking back at Eq. (1.24), the observation of constructive interference for a chosen scattering geometry (or scattering vector $\mathbf{K}$) clearly corresponds to a particular reciprocal lattice vector $\mathbf{G}$. The intensity measured at the detector is proportional to the square of the Fourier coefficient of the electron concentration $|\rho_{\mathbf{G}}|^2$. We could therefore think of measuring the intensity of the diffraction spots appearing for all possible reciprocal lattice vectors, obtaining the Fourier coefficients of the electron concentration and reconstructing this concentration from the coefficients. This would give us all the information needed and thus conclude the process of structure determination. Unfortunately, this straightforward approach does not work because the Fourier coefficients are complex numbers. Taking the square root of the intensity at the diffraction spot therefore gives the magnitude, but not the phase of $\rho_{\mathbf{G}}$. The phase is lost in the measurement; this is known as the **phase problem** in X-ray diffraction. To solve an unknown structure, one has to find a way to work around it. One simple approach for this is to calculate the electron concentration for a structural model, obtain the magnitude of the $\rho_{\mathbf{G}}$ values and thus also the expected diffracted intensity, and compare this to the experimental result. Based on the outcome, the model can be refined until the agreement is satisfactory.

In the following, we will describe in more detail how this can be achieved. We start with Eq. (1.11), the expression for the diffracted intensity that we had obtained before

introducing the reciprocal lattice. But now we know that constructive interference is only observed in an arrangement that corresponds to meeting the Laue condition and we can therefore write the intensity for a particular diffraction spot as

$$I(\mathbf{G}) \propto \left| \int_V \rho(\mathbf{r})\, \mathrm{e}^{-\mathrm{i}\mathbf{G}\cdot\mathbf{r}}\, \mathrm{d}V \right|^2. \tag{1.26}$$

We also know that the crystal consists of many identical unit cells at the positions $\mathbf{R}$ of the Bravais lattice. Therefore, we can split the integral and write it as a sum of integrals over the individual unit cells,

$$I(\mathbf{G}) \propto \left| \sum_{\mathbf{R}} \int_{V_{\mathrm{cell}}} \rho(\mathbf{r}+\mathbf{R})\, \mathrm{e}^{-\mathrm{i}\mathbf{G}\cdot(\mathbf{r}+\mathbf{R})}\, \mathrm{d}V \right|^2 = \left| N \int_{V_{\mathrm{cell}}} \rho(\mathbf{r})\, \mathrm{e}^{-\mathrm{i}\mathbf{G}\cdot\mathbf{r}}\, \mathrm{d}V \right|^2, \tag{1.27}$$

where N is the number of unit cells in the crystal and we have used the lattice periodicity of $\rho(\mathbf{r})$ and Eq. (1.14) in the last step. We now assume that the electron density $\rho(\mathbf{r})$ in the unit cell is given by the sum of atomic electron densities $\rho_i(\mathbf{r})$ that can be calculated from the atomic wave functions. In doing so, we neglect the fact that some of the electrons form bonds between the atoms and are no longer part of the spherical electron cloud around the atom. If the atoms are not too light, however, the number of these valence electrons is small compared to the total number of electrons and the approximation is appropriate. We can then write

$$\rho(\mathbf{r}) = \sum_i \rho_i(\mathbf{r} - \mathbf{r}_i), \tag{1.28}$$

where we sum over the different atoms in the unit cell (i.e. the basis) at positions $\mathbf{r}_i$. This permits us to rewrite the integral in Eq. (1.27) as a sum of integrals over the individual atoms in the unit cell

$$\int_{V_{\mathrm{cell}}} \rho(\mathbf{r})\, \mathrm{e}^{-\mathrm{i}\,\mathbf{G}\cdot\mathbf{r}}\, \mathrm{d}V = \sum_i \mathrm{e}^{-\mathrm{i}\,\mathbf{G}\cdot\mathbf{r}_i} \int_{V_{\mathrm{atom}}} \rho_i(\mathbf{r}')\, \mathrm{e}^{-\mathrm{i}\,\mathbf{G}\cdot\mathbf{r}'}\, \mathrm{d}V', \tag{1.29}$$

where $\mathbf{r}' = \mathbf{r} - \mathbf{r}_i$. The two exponential functions give rise to two types of interference. The first describes the interference between the X-rays scattered by the different atoms in the unit cell, and the second the interference between the X-rays scattered by the electrons within one atom. The last integral is called the **atomic form factor** and can be calculated from the atomic properties alone. We therefore see how the diffracted intensity for an assumed structure can be calculated from the atomic form factors and the arrangement of the atoms.

1.3.1.7 The Ewald Construction

In 1913, P. Ewald published an intuitive geometrical construction to visualize the Laue condition [Eq. (1.25)] and to determine the directions $\mathbf{k}'$ for which constructive interference is to be expected. The construction is shown in Figure 1.12, which represents a cut through the reciprocal lattice; the black points are the reciprocal lattice points. The construction works as follows:

1) We draw the wave vector $\mathbf{k}$ of the incoming X-rays such that it ends in the origin of the reciprocal lattice (we may of course choose the point of origin freely).

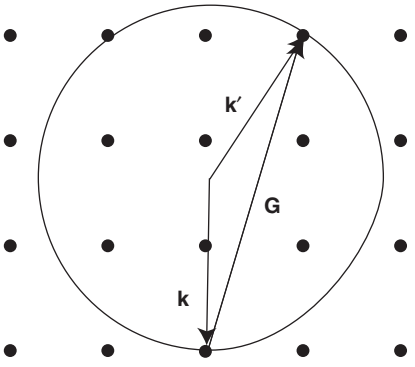

Figure 1.12 Ewald construction for finding the directions in which constructive interference can be observed. The dots represent the reciprocal lattice. The arrows labeled **k** and **k**′ are the wave vectors of the incoming and scattered X-rays, respectively.

2) We construct a circle of radius $|\mathbf{k}|$ around the starting point of $\mathbf{k}$.
3) Wherever the circle touches a reciprocal lattice point, the Laue condition $\mathbf{k}' - \mathbf{k} = \mathbf{G}$ is fulfilled.

For a three-dimensional crystal, this construction has to be carried out in different planes, of course. The figure clearly shows that Eq. (1.25) is a very stringent condition: It is not likely for the sphere to hit a second reciprocal lattice point, which means that constructive interference is expected for very few directions. As in the Bragg description, we see that the wavelength of the X-rays has to be sufficiently small ($|\mathbf{k}|$ has to be sufficiently large) for any constructive interference to occur.

Practical X-ray diffraction experiments are often carried out in such a way that many constructive interference maxima are observed despite the strong restrictions imposed by the Laue condition, Eq. (1.25). For example, this can be achieved by using a wide range of X-ray wavelengths, i.e. non-monochromatic radiation, or by performing a diffraction experiment not on a single crystal but on a powder of randomly oriented small crystals.

1.3.1.8 Relation Between Bragg and Laue Theory

We conclude our treatment of X-ray diffraction by showing that the Bragg description of X-ray diffraction is just a special case of the Laue description. We start by noting that the Laue condition in Eq. (1.25) consists, in fact, of three separate conditions for the three components of the vectors. In the Bragg experiment, two of these conditions are automatically fulfilled because of the specular geometry: The wave vector change parallel to the lattice planes is zero. So, the vector equation (1.25) reduces to the scalar equation

$$k'_{\perp} - k_{\perp} = 2k_{\perp} = 2\frac{2\pi}{\lambda}\sin\Theta = G_{\perp}, \tag{1.30}$$

where $G_{\perp}$ is a reciprocal lattice vector perpendicular to the lattice planes. We have seen in Section 1.3.1.4 that such a reciprocal lattice vector exists for any set of planes. The planes can be defined by their Miller indices (i, j, k) or by the reciprocal lattice vector $\mathbf{G}_{\perp} = i\mathbf{b_1} + j\mathbf{b_2} + k\mathbf{b_3}$ that is perpendicular to the planes (see Problem 1.9). The shortest possible $\mathbf{G}_{\perp}$ has a length of $2\pi/d$ with d being the distance between the planes, but any integer multiple of this will also work. Thus, if we insert $m\ 2\pi/d$ for $G_{\perp}$ into Eq. (1.30), we obtain the usual form of the Bragg condition in Eq. (1.3).

1.3.2 Other Methods for Structure Determination

While X-ray diffraction is arguably the most widespread and most powerful method for structure determination, other techniques are used as well. Similar diffraction experiments can be carried out by making use of the wave character of neutrons or electrons. The former interact very weakly with matter because they carry no electric charge. They are also more difficult to produce than X-rays. However, the use of neutrons has two distinct advantages over X-rays: First, their interaction with light atoms is stronger than that of X-rays, and second, they possess a magnetic moment, which means that they can interact with any magnetic moments in the solid, allowing one to determine its magnetic order. Electrons, on the other hand, have the advantages that they are easy to produce and that one can use electron-optical imaging techniques, whereas making optical elements for X-rays is very difficult. On the other hand, their very strong interaction with matter causes a breakdown of the kinematic approximation, that is, multiple scattering events have to be taken into account. Because of their strong interaction with matter, low-energy electrons do not penetrate deeply into crystals. Therefore, they are more appropriate for surface structure determination.

1.3.3 Inelastic Scattering

Our discussion has been confined to the case of elastic scattering. In real experiments, however, the X-rays or particles can also lose energy during the scattering events. This can be described formally by considering the diffraction from a structure that does not consist of atoms or ions at fixed positions but is time-dependent, that is, which fluctuates with the frequencies of the atomic vibrations. We cannot go into the details of inelastic scattering processes here, but it is important to emphasize that inelastic scattering, in particular of neutrons, can be used to measure the vibrational properties of a lattice.

1.4 Further Reading

The concepts of lattice-periodic solids, crystal structure, and X-ray diffraction are discussed in all standard texts on solid state physics, for example:

- Ashcroft, N.W. and Mermin, N.D. (1976). *Solid State Physics*. Holt-Saunders.
- Ibach, H. and Lüth, H. (2009). *Solid State Physics*, 4th edn. Springer.
- Kittel, C. (2005). *Introduction to Solid State Physics*, 8th edn. John Wiley & Sons
- Rosenberg, H.M. (1988). *The Solid State*. 3rd edn, Oxford University Press.

For a more detailed discussion of X-ray diffraction, see, for example:

- Als-Nielsen, J. and McMorrow, D. (2011). *Elements of Modern X-Ray Physics*, 2nd edn. John Wiley & Sons.

1.5 Discussion and Problems

Discussion

1.1 What mathematical concepts are used to describe the structure of any crystal?

1.2 What are the typical crystal structures of metals and why are they common?

1.3 Why do covalent crystals typically exhibit a much lower packing density than metallic crystals?

1.4 How can the reciprocal lattice conveniently be used to describe lattice-periodic functions?

1.5 How can the structures of crystals be determined?

1.6 What is the difference between the Bragg and von Laue descriptions of X-ray diffraction?

1.7 How can the reciprocal lattice of a crystal be used to predict the pattern of diffracted X-rays?

Basic Concepts

1.1 *Bravais lattice:* Figure 1.13 shows four two-dimensional lattices.

(a) Which of the following statements is true?

A. All four lattices are Bravais lattices.
B. Q is not a Bravais lattice.
C. Q and R are not Bravais lattices.
D. R is not a Bravais lattice.

(b) Draw the smallest possible unit cell of each lattice into the figure.

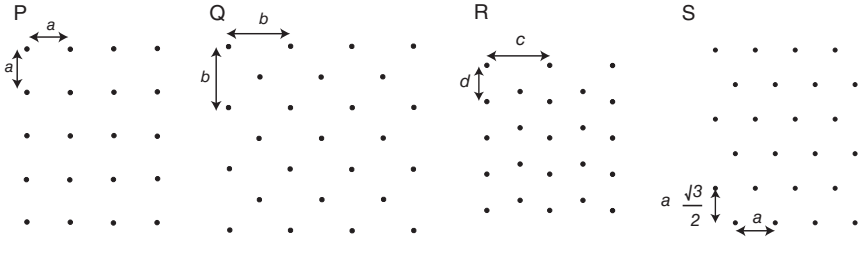

Figure 1.13 Two-dimensional lattices.

1.2 *Basis:*

(a) The left-hand side of Figure 1.14 shows a two-dimensional lattice with two types of atoms. We can think of the big white circles as nickel and the small grey ones as oxygen. When you describe this crystal by a two-dimensional Bravais lattice and a basis, how many atoms are there in the basis?

A. One.
B. Two.
C. Four.
D. Nine.

(b) The right-hand side of Figure 1.14 shows possible reciprocal lattices for this crystal. Which one is correct?

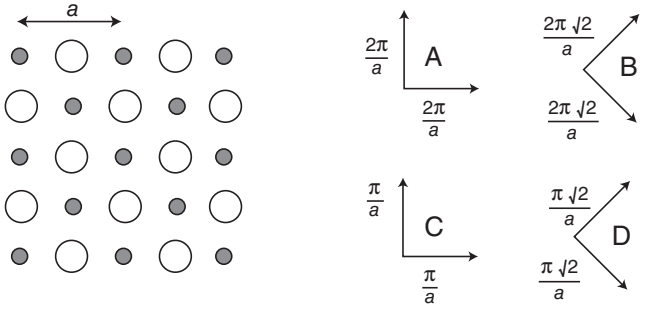

Figure 1.14 Left: two-dimensional NiO crystal; Right: possible choices of the reciprocal lattice for this crystal.

1.3 *Unit cell of a lattice:* Figure 9.6 shows a possible choice for the unit cell of barium titanate. The barium ions are located on the corners of the cube and the oxygen atoms on its faces. How many ions of the different types does this unit cell contain?

A. Ba: 4, Ti: 1, O: 4.
B. Ba: 8, Ti: 1, O: 6.
C. Ba: 1, Ti: 1, O: 3.

1.4 *The reciprocal lattice:* Consider a real-space Bravais lattice $\mathbf{R} = m\mathbf{a_1} + n\mathbf{a_2} + o\mathbf{a_3}$ and the corresponding reciprocal lattice $\mathbf{G} = m'\mathbf{b_1} + n'\mathbf{b_2} + o'\mathbf{b_3}$. Which of the following relations holds for all possible Bravais lattices?

A. $\mathbf{b_1}$ is parallel to $\mathbf{a_1}$.
B. $\mathbf{b_1}$ is perpendicular to the plane spanned by $\mathbf{a_1}$ and $\mathbf{a_2}$.
C. $\mathbf{b_1}$ is perpendicular to the plane spanned by $\mathbf{a_3}$ and $\mathbf{a_2}$.
D. $\mathbf{b_1}$ is perpendicular to $\mathbf{a_1}$.
E. None of the above.

1.5 *X-ray diffraction:* Which of the following can be determined from the positions of the spots in an X-ray diffraction pattern?
A. The reciprocal lattice.
B. The Bravais lattice.
C. Both A. and B.
D. The position of the atoms in the unit cell.
E. A., B., and D.

Problems

1.1 *Fundamental concepts:* For the two-dimensional crystal in Figure 1.15, find (a) the Bravais lattice and a primitive unit cell, (b) a nonprimitive, rectangular unit cell, and (c) the basis.

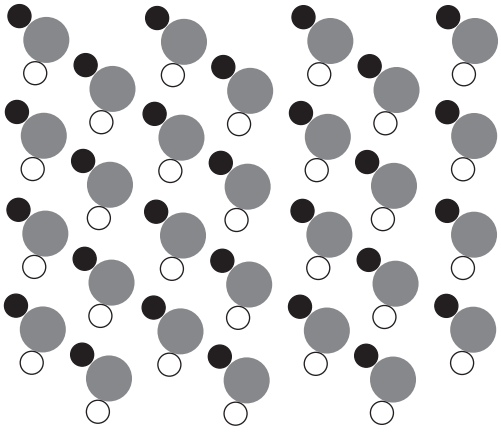

Figure 1.15 A two-dimensional crystal.

1.2 *Real crystal structures:* Show that the packing of spheres in a simple cubic lattice fills 52% of the available space.

1.3 *Real crystal structures*: Figure 1.16 shows the structures of a two-dimensional hexagonal packed layer of atoms, a hcp crystal, a two-dimensional sheet of carbon atoms arranged in a honeycomb lattice (graphene), and three-dimensional graphite. (a) Draw a choice of vectors spanning the Bravais lattice for the hexagonal layer of atoms and for graphene, and compare them to each other. (b) Show that the basis for the hexagonal layer contains one atom, while the bases for graphene and the three-dimensional hcp crystal contain two atoms. (c)***** Choose lattice vectors for the Bravais lattice of graphite and show that the basis contains four atoms.

1.4 *Real crystal structures:* Consider the hcp lattice shown in Figure 1.16b. The Bravais lattice underlying the hcp structure is given by two vectors of length a in one plane with an angle of 60° between them and a third vector of length

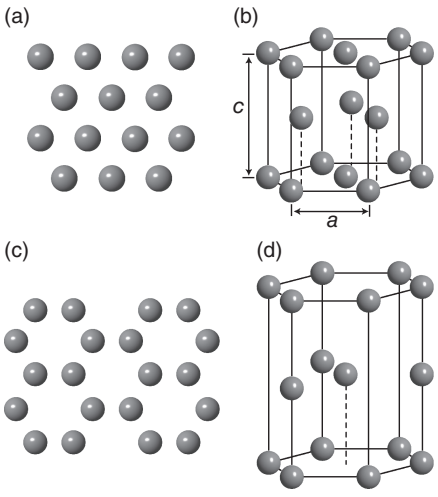

Figure 1.16 (a) Two-dimensional crystal structure of a hexagonal close-packed layer of atoms. (b) Crystal structure of a three-dimensional hcp crystal. (c) Two-dimensional crystal structure of graphene. (d) Three-dimensional crystal structure of graphite (strongly compressed along the *c* direction). The lines are a mere guide to the eye, not indicating bonds or the size of the unit cell.

c perpendicular to that plane. There are two atoms per unit cell. (a) Show that for the ideal packing of spheres, the ratio $c/a = (8/3)^{1/2}$. (b)* Construct the reciprocal lattice. Does the fact that there are two atoms per unit cell in the hcp crystal have any relevance? Hint: Use the result of Problem 1.7.

1.5 *X-ray diffraction:* (a) Determine the maximum wavelength for which constructive interference can be observed in the Bragg model for a simple cubic crystal with a lattice constant of 3.6 Å. (b) What is the energy of the X-rays in electron volts? (c) If you were to perform neutron diffraction, what kinetic energy would the neutrons need to possess for their de Broglie wavelength to be same? (d) One could argue that if one would use X-rays with twice the wavelength, one would still get a Bragg peak because then constructive interference would occur between the X-rays reflected from every other plane. Why is this argument not valid? (e) One could describe the same crystal by using a unit cell that is a bigger cube of twice the side length, containing eight atoms instead of one. The lattice constant would then be 7.2 Å. Discuss how this different description would affect the X-ray diffraction from the crystal.

1.6 *The reciprocal lattice:* Using the explicit definition of the reciprocal lattice in Eq. (1.16), show first that Eq. (1.17) is obeyed and then proceed, using this relation, to show that the reciprocal lattice defined by Eq. (1.16) does indeed meet the condition from Eq. (1.13).

1.7 *The reciprocal lattice:* For a two-dimensional Bravais lattice

$$\mathbf{R} = m\mathbf{a_1} + n\mathbf{a_2}, \tag{1.31}$$

the reciprocal lattice is also two-dimensional:

$$\mathbf{G} = m'\mathbf{b_1} + n'\mathbf{b_2}. \tag{1.32}$$

Often, the most practical way to construct the reciprocal lattice is to use the relation

$$\mathbf{a}_i \cdot \mathbf{b}_j = 2\pi\, \delta_{ij}, \tag{1.33}$$

which remains valid in the two-dimensional case. Find the reciprocal lattices for the three cases displayed in Figure 1.17.

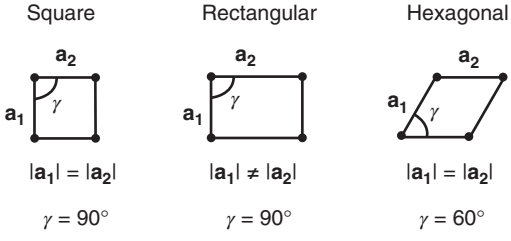

Figure 1.17 Two-dimensional Bravais lattices.

1.8 *Lattice-periodic functions:* Figure 1.11 shows two lattice-periodic functions and the Fourier coefficients generating these functions. The functions $\rho(x)$ have been calculated from the coefficients ρ_n using Eq. (1.20). (a) Write down the specific Fourier series corresponding to the lower half of Fig. 1.11 and make sure that the result is correct by plotting $\rho(x)$ in the same interval as in the figure, from $-5a$ to $5a$ (you may choose $a = 1$). (b) Now try the reverse operation by numerically calculating the Fourier transform of the obtained $\rho(x)$. Display the resulting $|\rho(k)|$. You will find that it does not match the right-hand side of Fig. 1.11: Instead of δ functions at the reciprocal lattice points, you will obtain quite broad peaks. Why is this so? What would be needed to narrow these peaks? Demonstrate how this can be achieved. (c)* Discuss the implications for the observed intensity in X-ray diffraction. To this end, note that upon fulfilling the Laue condition, the diffracted intensity around a reciprocal lattice vector as in Eq. (1.26) corresponds to the squared norm of the scattering density's Fourier transformation.

1.9 *Miller indices:* We have stated that the reciprocal lattice vector $m\mathbf{b_1} + n\mathbf{b_2} + o\mathbf{b_3}$ is perpendicular to the lattice plane given by the Miller indices (m, n, o). (a) Verify that this is correct for the lattice planes drawn in Figure 1.9. (b)* Show that this statement is universally valid.